

UCLA

UCLA Previously Published Works

Title

Network modeling suggests HIV infection phenocopies PI3K-AKT pathway mutations to enhance HPV-associated cervical cancer.

Permalink

<https://escholarship.org/uc/item/05s843v3>

Journal

Molecular Omics, 19(7)

Authors

Olwal, Charles
Fabius, Jacqueline
Zuliani-Alvarez, Lorena
[et al.](#)

Publication Date

2023-08-14

DOI

10.1039/d3mo00025g

Peer reviewed



Published in final edited form as:

Mol Omics. ; 19(7): 538–551. doi:10.1039/d3mo00025g.

Network modeling suggests HIV infection phenocopies PI3K-AKT pathway mutations to enhance HPV-associated cervical cancer

Charles Ochieng' Olwal^{a,b}, Jacqueline M Fabius^{c,d,e}, Lorena Zuliani-Alvarez^{c,d,e,f}, Eckhardt Manon^{c,d,f}, George Boateng Kyei^{g,h}, Peter Kojo Quashie^a, Nevan J Krogan^{c,d,e,f}, Mehdi Bouhaddou^{d,i,j,k}, Yaw Bediako^{a,l}

^aWest African Centre for Cell Biology of Infectious Pathogens (WACCBIP), University of Ghana, Accra, Ghana.

^bDepartment of Biochemistry, Cell and Molecular Biology, College of Basic and Applied Sciences, University of Ghana, Accra, Ghana.

^cThe J. David Gladstone Institute of Data Science and Biotechnology, San Francisco, CA, USA

^dQuantitative Biosciences Institute, University of California, San Francisco, CA, USA.

^eThe Cancer Cell Map Initiative, San Francisco and La Jolla, CA, USA

^fDepartment of Cellular and Molecular Pharmacology, University of California, San Francisco, CA, USA.

^gNoguchi Memorial Institute for Medical Research, College of Health Sciences, University of Ghana, Accra, Ghana.

^hUniversity of Ghana Medical Centre, University of Ghana, Accra, Ghana.

ⁱInstitute for Quantitative and Computational Biosciences (QCBio), University of California, Los Angeles, LA, USA.

^jDepartment of Microbiology, Immunology, and Molecular Genetics (MIMG), University of California, Los Angeles, LA, USA.

^kMolecular Biology Institute, University of California, Los Angeles, LA, USA.

^lYemaachi Biotech, Accra, Ghana.

coolwal@st.ug.edu.gh, ybediako@ug.edu.gh, Nevan.krogan@ucsf.edu, Bouhaddou@ucla.edu.

Author contributions

COO: Conceptualization, formal analysis, visualization, methodology and writing – original draft. JMF: resources and writing – review and editing. LZ: Conceptualization, review and editing. EM: Resources and methodology. GBK: Supervision and writing – review and editing. PKQ: Supervision and writing – review and editing. NJK: Funding acquisition, resources and writing – review and editing. MB: Conceptualization, funding acquisition, visualization, methodology, supervision, resources and writing – review and editing. YB: Conceptualization, funding acquisition, supervision and writing – review and editing.

Conflicts of interest

The Krogan Laboratory has received research support from Vir Biotechnology, F. Hoffmann-La Roche, and Rezo Therapeutics. NJK has previously held financially compensated consulting agreements with the Icahn School of Medicine at Mount Sinai, New York and Twist Bioscience Corp. He currently has financially compensated consulting agreements with Maze Therapeutics, Interline Therapeutics, Rezo Therapeutics, and GenIE Lifesciences, Inc. He is on the Board of Directors of Rezo Therapeutics and is a shareholder in Tenaya Therapeutics, Maze Therapeutics, Rezo Therapeutics, and Interline Therapeutics. MB is financially compensated scientific advisor for GenIE Lifesciences. COO, JMF, LZ, EM, GBK, PKQ and YB have no competing interests.

Abstract

Women coinfecting with human immunodeficiency virus type 1 (HIV-1) and human papillomavirus (HPV) are six times as likely to develop invasive cervical carcinoma compared to those without HIV. Unlike other HIV-associated cancers, the risk of cervical cancer development does not change when HPV/HIV coinfecting women begin antiretroviral therapy, suggesting HIV-associated immune suppression is not a key driver of cervical cancer development in coinfecting women. Here, we investigated whether the persistent secretion of inflammatory factors in HIV-positive patients on antiretroviral therapy could enhance cancer signaling in HPV-infected cervical cells via endocrine mechanisms. We integrated previously reported HIV-induced secreted inflammatory factors (Hi-SIFs), HIV and HPV virus-human protein interactions, and cancer patients genomic data using network propagation to understand the pathways underlying disease development in HPV/HIV coinfection. Our results pinpointed the PI3K signaling pathway to be enriched at the interface between Hi-SIFs and HPV-host molecular networks, in alignment with PI3K pathway mutations being prominent drivers of HPV-associated, but HIV independent, cervical cancer development. Furthermore, we experimentally stimulated cervical cells with 14 Hi-SIFs to assess their ability to activate PI3K-AKT signaling. Strikingly, we found 8 factors (CD14, CXCL11, CXCL9, CXCL13, CXCL17, AHSG, CCL18, and MMP-1) to significantly upregulate AKT phosphorylation (pAKT-S473) relative to a phosphate buffered saline control. Our findings suggest that Hi-SIFs cooperate with HPV infection in cervical cells to over-activate PI3K-AKT signaling and phenocopy PI3K-AKT pathway mutations to enhance cervical cancer development in coinfecting women. Our insights could support the design of therapeutic interventions targeting the PI3K-AKT pathway or neutralizing Hi-SIFs in HPV/HIV coinfecting cervical cancer patients.

Network modeling suggests the inflammatory factors secreted due to HIV infection, even in the presence of antiretroviral therapy, activate PI3K-AKT signaling in cervical cells and accelerate cervical cancer progression in HPV/HIV coinfecting women.

Introduction

Cervical cancer, primarily caused by persistent infection with certain human papillomavirus (HPV) types, remains a major global health burden. In 2020, over 300,000 cervical cancer deaths were reported, out of which approximately 90% were from Low-and-middle-income countries (LMICs)¹. Although cervical cancer is preventable through HPV vaccination as well as screening and treatment of pre-cancerous lesions², it is disproportionately higher in LMICs due to low coverage of preventative services, inadequate treatment of pre-cancerous lesions^{2,3} and late-stage detection⁴. Thus, effective screening, early detection and treatment strategies are crucial to ending the cervical cancer menace.

HPVs are sexually transmitted, epitheliotropic, non-enveloped viruses with approximately 7.9 kilobase circular double-stranded DNA genome. As of 8 April 2023, the International HPV Reference Center (<https://www.hpvcancer.se>) had recognized 229 HPV genotypes, out of which about 14 are classified as oncogenic high-risk (HR) types⁵. HPV infection is necessary but not sufficient for progression to invasive cervical carcinoma (ICC)⁶. Several cofactors, such as long-term use of oral contraceptives⁷, multiparity^{8,9}, infections e.g. Human immunodeficiency virus type 1 (HIV-1)¹⁰, Herpes simplex virus type 2¹¹ and

bacterial vaginosis agents¹² or genetic predisposition e.g. Human Leukocyte Antigen (HLA) allele polymorphisms (reviewed in^{13,14}), are often associated with the progression to ICC.

Women living with HIV have increased risk of persistent HR-HPV infection^{15,16}, a six times higher risk of developing cervical cancer (Fig. 1A;¹⁷), higher treatment failure rates¹⁸, elevated progression of pre-cancerous lesions to ICC,¹⁹ earlier onset of cancer² and reduced survival rates²⁰ compared to those without HIV. Intriguingly, although the introduction of antiretroviral therapy (ART) for HIV-infected women permits immune system rebound, their risk¹⁷ and incidence²¹ of progression to ICC remain elevated even when on ART (Fig. 1A–B). Despite other HIV/Acquired immuno-deficiency syndrome (AIDs)-defining cancers (i.e., Kaposi sarcoma and Non-Hodgkin (NH) lymphoma) declining dramatically in the post-ART era, cervical cancer occurrences have remained significantly stable^{21–24} (Fig. 1B). This trend implies that HIV-associated immune suppression is not the key mechanism underlying rapid progression to ICC in HPV/HIV coinfection. To this end, some efforts have been directed towards providing explanations for increased progression to cervical cancer in HPV/HIV coinfecting women. For instance, a study showed that HLA class II alleles (i.e., DQB1*03:01 and DQB1*06:02) are associated with cervical cancer development in HPV/HIV co-infected “Black South African” women.²⁵ In contrast, DQB1*06:02 was associated with protection against cervical cancer among Chinese women.²⁶ Furthermore, two studies limited to cell cultures have suggested that exposure to HIV transactivator (TAT) protein could enhance cervical cancer development.^{27,28} Thus, how HIV mechanistically contributes to elevated HPV-associated cervical cancer development is not fully understood and warrants further investigations. This information could provide insights for the design of more effective screening, detection and treatment options for cervical cancer in HPV/HIV coinfecting women.

To further probe the mechanistic contribution of HIV in enhancing HPV-associated cervical cancer development, we came up with three hypotheses (Fig. 1C). Previous reports have shown that HIV-infected individuals persistently over-express certain inflammatory factors regardless of the duration of and/or viral suppression levels by ART.^{29–31} Hence, our first hypothesis was that certain HIV-induced secreted inflammatory factors (Hi-SIFs) cooperate with HPV proteins to enhance cervical cancer development. Secondly, we hypothesized that HIV proteins directly impinge on cancer pathways of HPV-infected cervical cells to enhance cervical cancer development. This hypothesis was motivated by a previous study in which exposure of CaSki, an HPV16 positive cancer cell line, to exogenous TAT protein was shown to alter the expression patterns of HPV E6 and p53.²⁸ In this study, we sought to gain a more expanded understanding of how all HIV and HPV proteins converge on host pathways to accelerate cervical cancer development. Furthermore, a previous study suggested that HIV can enter cervical cells in a CD4-independent manner;³² therefore, our third hypothesis was that HIV could directly enter cervical cells and interact with HPV proteins to enhance cervical cancer development.

Here, we tested our first two hypotheses using network modeling, bioinformatics and statistical analysis. Specifically, we used a network modeling approach called network propagation, which uses a “guilt-by-association” approach to propagate signal through a network to identify interconnected neighborhood clusters or pathways.³³ We separately

performed network propagation of (i) Hi-SIFs known to be persistently over-expressed by HIV patients even when on ART relative to HIV-unexposed individuals,^{31,34–36} (ii) human proteins (“preys”) previously reported to physically interact with HPV (HPV-human PPIs), or (iii) HIV-human PPIs.^{37,38} We then integrated the HPV propagation outputs with those of either the Hi-SIF or HIV to study host pathways that converged between HIV and HPV. We focused our analysis by overlaying genomic data from cervical cancer patients curated in the cBioPortal for Cancer Genomics database (cBioPortal; <http://cbioportal.org>) onto the network propagation results to identify converging pathways relevant to cervical cancer (Fig. 1D). Our analyses reveal molecular network models whereby HIV cooperates with HPV to deregulate pathways associated with cell proliferation, migration, and immune evasion, leading to cervical cancer development and metastases.

Results

HPV preys, Hi-SIFs and HIV preys display poor overlap at the gene level

Our analysis revealed a poor overlap of the HIV preys, Hi-SIFs and HPV preys at the gene level (Fig. 1E). Preliminary gene set enrichment analysis (GSEA) on these genes (Hi-SIFs, HIV only, HPV only, or HIV-HPV overlapping) pointed to translation, cell cycle, and ubiquitin-mediated proteolysis as converging between HIV and HPV (Fig. 1F and Table S1). Although intriguing, this analysis could not provide enough granularity into how HPV preys, Hi-SIFs, and HIV preys converged into physical and functional interaction networks to cooperatively hijack these processes.

Network propagation analysis highlights host pathways co-opted by HPV and HIV during cervical cancer development

To achieve network-level understanding of how sets of HPV preys and Hi-SIFs or HIV preys are interconnected, we performed network propagation. This approach simulates a heat diffusion process to propagate a signal from genes of interest (“seed nodes”) to neighboring genes, connected based on prior physical and functional interactions between proteins. This process expands a set of genes into the molecular networks in which they participate. We used Pathway Commons for our base network, which is a combination of both physical and functional interaction networks. We performed three independent network propagations, using either the (i) Hi-SIFs (n=26), (ii) HIV (n = 241) or (iii) HPV (n = 356) genes as the initial seed sets, labeling all ‘seed’ nodes 1 and all other nodes 0. We performed a permutation test to identify nodes receiving more “heat” than would be expected by chance (see Materials and methods). To integrate propagated networks, we selected genes that were significant ($p < 0.05$) for both HPV and Hi-SIFs (n = 393; Fig. 2A) or for HPV and HIV (n = 500) propagations (Fig. S2A). This analysis was designed to favor genes with high propagation scores (i.e., lowest p -values) from each pair of propagations, thus identifying molecular networks that overlap between the initial seed sets. Following integration, we induced a subnetwork of these significant genes from our original base network and sub-clustered it into smaller subnetwork pieces. This resulted in 19 (Fig. 2A and Fig. S1) and 33 (Fig. S2A and Fig. S3) smaller HPV/Hi-SIFs and HPV/HIV subnetwork clusters, respectively, to ease visualization and interpretation.

To select the subnetwork clusters of our propagated networks most relevant to cervical cancer, we assessed the alteration frequencies of genes within each subnetwork cluster (including point mutations, copy number alterations (CNA), as well as mRNA and protein up or down-regulation) among cervical cancer patients from two studies, including Cervical Squamous Cell Carcinoma (TCGA, PanCancer Atlas) and Cervical Squamous Cell Carcinoma and Endocervical Adenocarcinoma (TCGA, Firehose Legacy), curated in cBioPortal (Fig. 2B). Pathway enrichment analysis on each of the resulting subnetwork clusters highlighted host pathways associated with each of the 19 Hi-SIFs/HPV subnetwork clusters (Fig. 2C and Table S2). The top five altered clusters (i.e., 9, 10, 13, 14 and 15; Fig. 2B–D) were implicated in phosphoinositide 3-kinase (PI3K)-AKT and ErbB signaling, DNA damage response, and Rho GTPase signaling (Fig. 2C). We next sought to determine if cervical cancer development in general was associated with the above pathways. We observed that the alteration frequencies of genes in these subnetwork clusters were more commonly altered in cervical cancer than in other cancers common in women (<https://gco.iarc.fr/>; Accessed on 1st July 2022), including breast, stomach, colorectal, lung and liver (Fig. 2E). Similarly, the alteration frequency of the PIK3CA gene (the catalytic subunit of PI3K) was highest in cervical cancer relative to other five cancers common among women (Fig. 2F). We also noted that PIK3CA is the second most frequently mutated gene in cervical cancer (Fig. 2F, inset). Collectively, these analyses underscored the essentiality of PI3K-AKT pathway in cervical cancer development. Next, we asked whether Hi-SIFs, HIV or HPV can independently affect PI3K-AKT signaling pathway. To answer this question, we extracted the top 500 significant genes from each of the datasets (i.e., HPV preys, Hi-SIFs and HIV preys propagation outputs) and induced them into a network followed by clustering into subnetwork clusters. GSEA of the resultant subnetwork clusters revealed that Hi-SIFs impinge on PI3K-AKT pathways (Fig. 2G and Table S3–5). This suggests that Hi-SIFs could phenocopy PI3K-AKT pathway mutations in HPV-associated cervical cancer progression.

We next performed the same analysis comparing the HPV and HIV propagations. A GSEA of the 33 HIV/HPV propagated subnetwork clusters (Fig. S2A and Fig. S3) revealed host pathways that might be co-hijacked by these viral pathogens to drive cervical cancer. To unbiasedly select subnetwork clusters that are likely to be linked to cervical cancer development, we plotted mutation frequencies for genes within each subnetwork cluster and selected the top five most frequently altered clusters (Fig. S2B). The top five most frequently altered clusters (16, 23, 30, 32 and 33) were implicated in mRNA splicing, pre-mRNA processing, transcriptional regulation by TP53, and homologous-directed repair through single-strand annealing (HDR-ssa; Fig. S2C and Table S6). Next, we assessed if these pathways were more frequently altered in cervical cancer compared to other common cancers among women. To achieve this, we pulled out the nodes from the top five altered clusters (Fig. S2D) and annotated their alteration frequencies across various cancers (Fig. S2E). We found cervical cancer to be ranked first for mRNA splicing and 2nd for HDR-ssa. These analyses suggest that mRNA splicing and processing are implicated in cervical cancer development and may be pathways hijacked by HPV and HIV coinfection.

HPV, HIV and cervical cancer genomics converge on PI3K-AKT signaling, mRNA splicing and cell cycle pathways

Nearly all cervical cancer cases originate from HPV infection. HPV infection is often accompanied by other somatic mutations that accrue, accelerated by the disruption of p53, which can drive progression to advanced cervical cancer. We asked if any of these somatic mutations occurred on the HIV-induced Hi-SIFs or HIV preys, raising the possibility that HIV could “mimic” a somatic cancer driver mutation through pathway regulation or by directly interacting with a host protein. For example, the same functional outcome could result from a somatic mutation disrupting the catalytic activity of a tumor suppressor and an inflammatory factor activating a pro-cancer pathway. To assess this, we first extracted and ranked the mutation and CNA frequencies of Hi-SIFs or HIV preys across different cervical cancer grades and stages from the cBioPortal as detailed in Fig. S4A. For Hi-SIFs, C3, SLAMF1, CD163, CCL23, AHSB, MMP1, APOA1 and IL6 emerged as the top mutated proteins among cervical cancer patients (Fig. 3A) whereas HUWE1, ANKHD1, RANBP2, EPPK1, DNAJB11, RNF7 and PLOD2 were the most frequently mutated HIV preys during cervical cancer development (Fig. S5A). We next wanted to understand how these top proteins were interconnected with our subnetwork clusters. Because network clustering essentially removes edges, we added back any edges between a subnetwork cluster and one of these top candidate proteins (Figs 3B, S4A and S5B). We then performed GSEA on propagated subnetwork clusters with at least one connection to any of the top mutated Hi-SIFs or HIV preys. In line with our Hi-SIFs/HPV propagated subnetwork clusters (Fig. 2C), the top mutated Hi-SIFs interconnected with subnetwork clusters implicated in PI3K-AKT signaling and DNA damage response (Fig. 3C and Table S7). Indeed, the centrality of PIK3CA mutations in cervical cancer development is well established even in the absence of HIV.^{39–42} Thus, we wondered whether HIV infection enhances cervical cancer development via directly increasing PIK3CA mutations. Interestingly, a recent Ugandan genomics study revealed that a higher proportion of HIV-negative cervical tumors had PIK3CA mutation compared to the HIV-positive tumors (Fig. 3D)⁴³, suggesting that HIV could rather be phenocopying the PI3K-AKT pathway mutations to accelerate HPV-associated cervical cancer development.

We also noted that the top mutated HIV preys connected to subnetwork clusters implicated in mRNA splicing, pre-mRNA processing, and cell cycle (Fig. S5C and Table S8) in line with HPV/HIV propagated network outputs (Fig. S2C). In addition, when we checked the alteration frequencies of our top 10 significant proteins with the terms “splicing” from our HPV/HIV network propagation (Table S6), we noted that these proteins are altered (i.e., point mutations, CNA and structural variants, mRNA and protein expression) in 63% of the cervical cancer patients listed in cBioPortal (Fig. S5D). This further suggested that mRNA splicing is a key cervical cancer pathway.

Mechanistic models of HPV/HIV cooperation in cervical cancer development

Our analyses above pointed to PI3K-AKT as a pathway that is co-hijacked by Hi-SIFs and HPV proteins. Since physical and functional interaction is an indicator of whether two or more proteins are involved in the same pathway(s), we first decided to check how the Hi-SIFs were interconnected with PI3K-related genes from our network propagation. To

(i.e., conjugation of a ubiquitin-like protein, NEDD8, to target proteins). The activated E3 ligases likely ubiquitinate cellular splicing proteins and target them for proteasomal degradation, which would reduce the levels of certain protein isoforms produced. On the one hand, if the splicing proteins targeted are tumor suppressors, this may cause a decrease in their levels consequently interfering with regulation of cell cycle progression. On the other hand, deregulated mRNA splicing may lead to formation of a variant form of a protein (e.g., MHC class I proteins) thereby hampering recognition and clearance of the cancerous cells by the immune system. This model is supported by previous studies showing that HPV proteins, such as E2, regulate splicing factors⁴⁷ and could promote the production of cell mRNA variants and proteins with oncogenic functions leading to cervical cancer development (reviewed in⁴⁸). Altogether, the deregulation of the mRNA splicing by the two viral pathogens could lead to aberrant cell cycle and immune evasion thereby promoting cervical cancer progression and metastases.

Discussion

High HIV prevalence is correlated with HPV-associated cervical cancer burden.¹⁷ HIV-induced immune suppression has been viewed as the mechanism underlying faster cervical cancer progression among HIV/HPV coinfecting women. However, unlike other HIV/AIDS defining cancers, the introduction of ART has not significantly reduced cervical cancer incidences.^{21–24} Although it could be argued that immune suppression irreversibly triggers cervical carcinogenesis pre-ART, there is still inconclusive and conflicting evidence on the impact of baseline or nadir CD4 counts on cervical cancer progression.^{49–52} Considering this, immune suppression does not appear to be a key mechanism underlying cervical cancer progression. Thus, we wondered how HIV contributed to increased HPV-associated cervical cancer progression. Here, we harnessed network modeling to reveal several candidate molecular pathways underlying HIV/HPV cooperation in enhancing cervical cancer development.

Our analyses highlighted that HIV and HPV co-hijack PI3K-AKT and ErbB signaling, DNA damage response, Rho GTPase, mRNA splicing, pre-mRNA processing, transcriptional regulation by TP53, and HDR-ssa. Most of these pathways have been strongly associated with development of cancers, including cervical cancer, due to their direct effect on cell proliferation, migration, immune evasion or genomic stability.^{53–56} It has been reported that concomitant deregulation of cancer pathways, such as p53 and RB1 pathways, have more drastic effect on cervical cancer progression than deregulation of only one of the pathways.^{57–59} Thus, it is plausible that the cooperative deregulation of the pathways identified in our analysis by both HIV and HPV could be responsible for the enhanced progression to advanced cervical cancer and metastasis usually reported among dual HIV and HPV infected women. Our findings are in agreement with previous studies that highlighted the importance of some of the pathways revealed by our network modeling, including PI3K-AKT signaling,⁶⁰ mRNA splicing⁶¹ and DNA damage response,⁶² in cervical cancer development.

Furthermore, our analysis revealed that nodes associated with PI3K-AKT and mRNA splicing are more altered among cervical cancer patients relative to other common cancers

among women, including breast, stomach, colorectal, lung, and liver cancer. This suggests these pathways to be central drivers of cervical cancer. PI3K signaling and mRNA splicing are also implicated during HIV pathogenesis particularly during viral entry, latency, reactivation, and viral spread, as previously discussed^{63,64}. The essentiality of these pathways in HIV pathogenesis implies that they are prone to deregulation during HIV infection. Similarly, HPV infection is frequently associated with mutations of PIK3CA,^{39,43} a key node in the PI3K-AKT signaling pathway. Thus, it is highly likely that there is cooperative deregulation of the PI3K-AKT signaling by HPV and HIV infections leading to elevated cervical cancer progression in coinfecting women.

Based on the observed essentiality of PI3K-AKT signaling and mRNA splicing in HIV-HPV pathogenesis and cervical cancer, we propose an indirect and direct models of HPV/HIV cooperation in elevating cervical cancer development. In the indirect model, Hi-SIFs activate PI3K-AKT pathway nodes leading to aberrant cell proliferation and migration. In the direct model, HIV hijacks and activates E3 ubiquitin ligases, which in turn enhances ubiquitination and proteasomal degradation of splicing factors. The altered mRNA splicing may interfere with the abundance and variety of protein isoforms produced. Aberrant ubiquitination of splicing proteins could deplete tumor suppressors leading to uncontrolled cell proliferation or create variant forms of proteins that could interfere with immune recognition and destruction of cancerous cells. It is possible that HIV utilizes both mechanisms (indirect and direct) to accelerate cervical cancer development. It remains unclear whether HIV is involved during early, late, or both early and late stages of cancer development. Our findings suggest that HIV could be implicated in multiple stages of cervical cancer development. This may partly explain why reduced HIV viral loads or rebound of the CD4+ T cells following ART treatment do not lessen the risk of progression to advanced cervical cancer. However, further studies are needed to unravel the precise stage(s) in which HIV is implicated.

From the cervical cancer patients genomic data, we noticed that the top mutated Hi-SIFs and HIV preys were strongly associated with nearly all the grades and stages of cervical cancer. These observations suggest two scenarios depending on which of the virus infects first or whether there is concurrent viral infection. In the first scenario, HIV promotes and augments HPV oncogenic activities throughout cervical cancer development phases. This is likely to occur if patients contract HIV before HPV or contract the two viruses concurrently. In the second scenario, mutations strongly associated with stage 4 cervical cancer, such as HUWE1 and EPPK1, could be secondary mutations that cause cells with already established HPV infection to progress to advanced disease. This second scenario is plausible where patients are typically infected with HPV prior to being infected with HIV, suggesting that HPV provokes oncogenesis and HIV triggers progression to advanced disease. More studies will be required to unravel which of these scenarios is common.

Our experimental data showed that several Hi-SIFs, namely CD14, CXCL11, CXCL9, CXCL13, CXCL17, AHSN, CCL18 and MMP-1, activate PI3K-AKT signaling. The present findings agree with previous studies on other cancers in which CXCL13,⁶⁵ CXCL9,⁶⁶ CCL18⁶⁷ were shown to upregulate PI3K signaling. Since HPV proteins are already known to deregulate PI3K-AKT signaling,^{44,45} our findings suggest that in the HPV/HIV

coinfection, there is cooperative deregulation of PI3K-AKT signaling. This concerted deregulation of PI3K-AKT signaling could enhance cervical cancer development in two ways. One, activation of PI3K signaling could increase cell proliferation and migration. Two, HIV and HPV-associated PI3K-AKT signaling activation could enhance immune evasion by the cervical cells leading to rapid cancer development. The second view is supported by a previous study in which activation of PI3K signaling was shown to promote immune evasion via reducing the expression of T-cell-attracting chemokines and CD8⁺ T-cell infiltration.⁶⁸ Even though HPV and HIV may infect concurrently or at different times, our study did not unravel the precise nature of cooperation (i.e., competitive, synergistic, additive etc.) between HPV and HIV in the deregulation of PI3K-AKT signaling pathway. Further studies will be required to discern the nature of their cooperation. In addition, future studies will be necessary to determine whether the deregulation of PI3K-AKT signaling by HPV and Hi-SIFs occur simultaneously or at separate phases of cervical cancer development.

In summary, this is the first comprehensive HIV and HPV network modeling analysis providing insights into possible mechanistic pathways, including PI3K-AKT signaling, ErbB signaling, DNA damage response, Rho GTPase, mRNA splicing, pre-mRNA processing, and HDR-ssa, underlying faster progression to advanced cervical cancer in the context of HPV/HIV dual infection. Specifically, our network modeling and experimental data pinpointed that the HIV-induced over-expression of certain inflammatory factors activate PI3K-AKT signaling pathway, which is already known to be deregulated by HPV infection. In addition, our analyses suggested that HIV and HPV proteins could be cooperating to deregulate mRNA splicing and processing. The cooperative deregulation of PI3K-AKT signaling pathway and mRNA splicing by HIV and HPV infections could be underlying the elevated cervical cancer development in HPV/HIV coinfecting women. However, we acknowledge that cancer pathogenesis, including cervical cancer, is a complex and multifactorial process⁶⁹ that cannot be limited to PI3K-AKT signaling and/or mRNA splicing pathways. More studies will be required to unravel additional pathways and/or factors that might be contributing to the rapid cervical cancer development seen in HPV/HIV dual infected women. We anticipate that our ongoing clinical studies in HIV-endemic areas of sub-Saharan Africa and other future molecular studies by other researchers will corroborate the present findings and interrogate the role of the other molecular pathways revealed by our network modeling to be co-opted by HIV and HPV infections in cervical cancer development. A better understanding of the mechanisms of HPV/HIV cooperation in cervical cancer development could inspire the design of effective therapeutic interventions targeting the key pathways implicated, ultimately speeding up cervical cancer elimination.

Materials and methods

Network propagation

To assess the network connectivity between HPV-human interacting proteins and either Hi-SIFs or HIV-human interacting proteins, we performed an integrative network propagation analysis. For our initial seed set, we used 26 Hi-SIFs extracted from the literature^{31,34–36} and previously reported AP-MS-generated HIV³⁸ and HPV³⁷ preys. We used Pathway Commons

as base network, subsetting for Reactome functional interactions (FI), CORUM, and physical interactions (Table S9), we performed diffused (heat) kernel network propagation to capture the local topology of the interaction network. This process is depicted by the equation below:^{70,71}

$$d = h * \exp(-Lt)$$

Where, h is a vector representing the original query, d is the resulting propagation results vector, L is the the graph Laplacian defined by $D - A$, (where D is the diagonal matrix holding the degree of each node and A = graph adjacency matrix of the input network; t = total time of diffusion - controls the extent to which the original signal is allowed to spread over the network. Default t was set at 0.1. The $\exp(*)$ stands for the matrix exponential.

Network propagations were performed separately for Hi-SIFs, HIV and HPV preys. In the first propagation, genes were labeled (1 or 0) if they were Hi-SIFs. In the second and third propagations, genes were labeled (1 or 0) if they were HPV or HIV preys, respectively. To control for nodes with many connections, which are biased to receive higher propagation scores due to their high connectivity, a permutation test was performed. Specifically, we simulated “random propagations” by shuffling the initial gene labels to random genes within the network 10,000 times. Next, we obtained an empirical p -value (Table S10) by calculating the fraction of random propagation runs greater than or equal to the true propagation run for each gene. Pairs of propagated networks were integrated by selecting genes that were significant in two propagations (i.e., HPV versus Hi-SIFs or HPV versus HIV).

A network was created by extracting a subgraph from the Pathway Commons network corresponding to the top significant ($p < 0.05$) genes from the integrative HPV/Hi-SIFs ($n = 393$) and HPV/HIV ($n = 500$) propagation ranked by their empirical p -values.

Clustering of propagated network

To identify the host pathways associated with Hi-SIFs, HIV and HPV, we clustered the propagated HPV/Hi-SIFs or HPV/HIV network into subnetwork clusters followed by GSEA. We initially visualized the network using Cytoscape version (v)3.9.1 and clustered it into subnetwork clusters using Glay community⁷² – a widely used Cytoscape plugin. However, we obtained a few large subnetwork clusters with broad pathway terms. Thus, we opted to explore an alternative clustering approach built around `cluster_walktrap`, a function on `igraph` package v1.3.5⁷³ and/or `cutreeDynamic`, a function on `dynamicTreeCut` package v1.63–1.⁷⁴ In brief, our alternative network clustering approach had two layers. In the first layer, the propagated network was clustered into subnetworks using `cluster_walktrap` function from the `igraph`⁷³ package in R, with 10 steps and transformed into an `hclust` object. The distance between nodes were calculated and normalized using the `cophenetic` function in R. Next, the resultant subnetworks were further clustered using `cutreeDynamic` function with the `minClusterSize` and `deepSplit` arguments set to 7 and 4, respectively. Upon clustering the propagated integrative HPV/Hi-SIFs or HPV/HIV network, GSEA was performed using `clusterProfiler` package v4.4.1.⁷⁵

Integration of cervical cancer patients' genomic data

cBioPortal (<http://cbioportal.org>) is a publicly available web resource for exploring, visualizing, and analysing multidimensional cancer genomics datasets drawn from several cancer patients.^{76,77} The cBioPortal also contains clinical data of the patients. We utilized data from two cervical cancer studies, namely the Cervical Squamous Cell Carcinoma (TCGA, PanCancer Atlas; n = 297) and Cervical Squamous Cell Carcinoma and Endocervical Adenocarcinoma (TCGA, Firehose Legacy; n = 310), listed in cBioPortal.

To identify the Hi-SIFs and HIV preys most likely implicated in cervical cancer development, we extracted and analyzed the clinical and genomic data from the two cervical cancer studies. In brief, we first downloaded the clinical data for the two cervical cancer studies from cBioPortal. Next, we extracted the cervical cancer patients' identification numbers (IDs) corresponding to each of the cancer grades (i.e., grade I to grade III). The TCGA, Firehose Legacy study contained both the International Federation of Gynecology and Obstetrics (FIGO) and tumor, nodes and metastases (TNM) cancer staging systems whereas TCGA, PanCancer Atlas study provided only TNM cancer staging system. Thus, for uniformity, we opted for TNM staging system to extract patients' IDs corresponding to stage 1 (sub-stage: T1, T1a, T1a1, T1a2, T1b, T1b1, T1b2, T1b3); stage 2 (sub-stage: T2, T2a, T2a1, T2a2, T2b); stage 3 (sub-stage: T3, T3a, T3b) and stage 4 (sub-stage: T4, M1) from both studies. The patient IDs for the sub-stages were merged to obtain the IDs for the four main stages (i.e., stage 1–4). The patients IDs for each of the cervical cancer grades and stages were used to filter for mutation and copy number alterations (CNA) data from the two cervical cancer studies in the cBioPortal. The extracted mutation and CNA data together with a list of Hi-SIFs or HIV preys were loaded onto R software for further analysis. In the analysis, mutation and CNA data were obtained only for cervical cancer patients whose cervical cancer grades and/or stages information were available for TCGA, Firehose Legacy and TCGA, Pancancer Atlas studies (Fig. S4B).

To extract mutation and CNA frequencies for the Hi-SIFs or HIV preys per grade or stage, we matched the mutation or CNA frequency data downloaded from cBioPortal to the list of Hi-SIFs or HIV preys. The average (for the two cervical cancer studies) mutation or CNA frequencies for Hi-SIFs or HIV preys per grade or stage were computed. In instances where one of the studies did not have a frequency entry for a particular Hi-SIFs or HIV prey, the available frequency value was used without averaging. Heatmaps showing variations of mutation or CNA frequencies of the HIV preys across cervical cancer grades and stages were prepared using ComplexHeatmap package v2.12.0.⁷⁸ The average values of the heatmap rows (denoting Hi-SIFs or HIV preys) were ranked in descending order based on the average mutation or CNA frequencies calculated across the grades or stages. The top three mutated Hi-SIFs or HIV preys per heatmap were selected for integration into the respective propagated networks (Fig. 3A–B and Fig. S5A–B). This integration involved re-visiting each of the Hi-SIFs/HPV or HIV/HPV propagated network clusters to add nodes corresponding to the top mutated Hi-SIFs or HIV preys, respectively. These nodes were added if there was a connection within the Pathway Commons network between any member of the subnetwork cluster and the top mutated Hi-SIFs (pink edges; Fig. 3B) or HIV prey (blue edges; Fig. S5B).

Gene set enrichment analysis

To understand the pathways associated with the subnetwork clusters from our networks, we performed GSEA using ClusterProfiler package v4.4.1. We simplified terms using a custom method, involving calculating term similarity based on gene membership, clustering terms accordingly, and cutting the dendrogram at a certain height (0.8 in our case). We selected the most general term to represent each clustered group of terms. Only significant terms (p -adjusted value < 0.05) were selected. The resulting enrichment map was visualized using ComplexHeatmap package v2.12.0 in R.

Network visualization

We formed networks in R using `graph_from_data_frame` function from `igraph` package v1.3.5. Networks were then visualized using `create_layout` and `ggraph` function from `ggraph` package v2.1.0. Apart from the Hi-SIFs/PI3K genes network (Fig. 4A) that was visualized in Cytoscape v3.9.1, all the other networks were visualized in RStudio.

Cell lines and in-cell western blot assay

The human cervical carcinoma cell line C33A⁷⁹, obtained as a gift from Jacques Archambault, McGill University, Canada, was maintained in Dulbecco's Modified Eagle Medium (DMEM) with 10% fetal bovine serum (FBS, Gibco) and 1% penicillin/streptomycin (Corning). This cell line was validated in 2017 by STR analysis using the GenePrint 10 assay (Promega) at the University of California, Berkeley Cell Culture Facility³⁷.

As summarized in Fig. 4B, activation of PI3K-AKT signaling (using phosphorylation of pAKT-S473 as proxy) upon stimulation of the C33A cells with different Hi-SIFs was evaluated using in-cell western blot assay as described previously⁸⁰ with some modifications. In brief, $\sim 5 \times 10^4$ C33A cells were seeded into a black walled clear bottom 96-well plates (Corning #3904) for about 24 hours at 37°C with 5% CO₂. Cells were then washed twice with 1X phosphate buffered saline (PBS) before addition of 198 μ L of serum-free DMEM and incubation at 37°C for 16 hours. Two μ L of each of the Hi-SIFs (50 ng/mL, Peprotech) or 1X PBS (control) was added to the respective wells and mixed gently followed by incubation at 37°C for 30 or 60 minutes. The cells were then fixed using 150 μ L of 4% of paraformaldehyde (PFA) solution (Thermo Fisher # PI28908) for 20 minutes at room temperature. The PFA was gently removed and each well washed three times with 200 μ L of 1X PBS. Cells were permeabilized using 50 μ L of 1:100 dilution of Triton X-100 (Sigma #9002-93-1) in 1X PBS for 30 minutes. Next, permeabilization buffer was removed, 50 μ L of blocking buffer (LI-COR, P/N 927-70001) added and incubated at room temperature for 2 hours. The blocking buffer was removed and replaced with 50 μ L of 1X primary antibodies, prepared by diluting total AKT (mouse; Cell Signaling Technologies #2920S) and pAKT-S473 (rabbit; Cell Signaling Technologies #4060S) at 1:1000 dilution in the blocking buffer. Cells were incubated in 50 μ L of 1X primary antibody solution overnight at 4°C in the dark with gentle rocking. The following morning, cells were washed with 200 μ L per well of 1X wash buffer (500 μ L Tween-20 in 1000 mL of 1X PBS) three times and rinsed once with 200 μ L per well of 1X PBS. Then, 50 μ L of 1X secondary antibody solution containing 1:1000 dilution of near infrared anti-mouse (926-32210) and anti-rabbit

(926–32211) antibodies was added per well followed by incubation for 2 hours in the dark at room temperature with gentle rocking. Cells were washed three times using 200 μ L/well of 1X wash buffer and rinsed once with 1X PBS. A 100 μ L of PBS was added to each well prior to fluorescence detection using LiCOR Odyssey plate scanner (9140). Wavelengths for the antibodies were set to 680 and 800 nm for anti-rabbit and anti-mouse, respectively. The focus distance was set at 4 mm and scanning performed at 169 μ m resolution. Raw signal intensities per well were analyzed using Image Studio software v5.2.5 (LI-COR, Inc.)

Bioinformatics and statistical analysis

All analyses were conducted with open-source resources. Analyses and visualization were performed using various packages anchored on R v4.2.3 (R Development Core Team, Vienna, Austria) and RStudio v2023.03.0+386 as detailed in the preceding sections. All the figures were transferred to Adobe Illustrator 2023 for final visualization.

Supplementary Material

Refer to Web version on PubMed Central for supplementary material.

Acknowledgements

Charles Olwal was supported by a WACCBIP-World Bank ACE PhD fellowship (WACCBIP+NCDs: Awandare). This research was further supported by a grant from the University of California, San Francisco Global Cancer Program at the Helen Diller Family Comprehensive Cancer Care Center (Global Cancer Pilot Award). This research was also funded by grants from the National Institutes of Health (P50AI150476, U54AI170792, U54CA209891, U54CA274502 to NJK and F32CA239333 and K99AI163868 to MB); by the Excellence in Research Award (ERA) from the Laboratory for Genomics Research (LGR), a collaboration between UCSF, UCB, and GSK (#1331222P); by the James B. Pendleton Charitable Trust; and by funding from F. Hoffmann-La Roche and Vir Biotechnology.

Data availability

The datasets generated and/or analysed during the current study and the codes are available in the GitHub repository, https://github.com/olwalco/Network_modeling_HIV_HPV and its supplementary files.

References

1. Sung H, Ferlay J, Siegel R, Laversanne M, Soerjomataram I, Jemal A and Bray F, CA Cancer J Clin, 2021, 71, 209–249. [PubMed: 33538338]
2. WHO, Cervical cancer, <https://www.who.int/news-room/fact-sheets/detail/cervical-cancer>, (accessed 7 October 2022).
3. Dzinamarira T, Moyo E and Dzobo M, Int J Gynecol Cancer, 2022, 0, 1–6.
4. Stewart TS, Moodley J and Walter FM, Cancer Epidemiol, 2018, 53, 81–92. [PubMed: 29414636]
5. Bouvard V, Baan R, Straif K, Grosse Y, Secretan B, El Ghissassi F, Benbrahim-Tallaa L, Guha N, Freeman C, Galichet L, Coglianò V, and WHO International Agency for Research on Cancer Monograph Working Group, Lancet Oncol, 2009, 10, 321–322. [PubMed: 19350698]
6. Meites E, Gee J, Unger E and Markwitz L, in Epidemiology and prevention of vaccine-preventable diseases: The Pink Book, eds. Hall E, Wodi A, Hamborsky J, Morelli V and Schillie S, Public Health Foundation, Washington, D.C, 14th edn., 2021, pp. 165–178.
7. Herrero R and Murillo R, in Cancer Epidemiology and Prevention, eds. Thun M, Linet MS, Cerhan JR, Haiman CA and Schottenfeld D, Oxford University Press, 4th edn., 2017, pp. 925–946.

8. Kim J, Kim BK, Lee CH, Seo SS, Park S-Y and Roh J-W, *Int J Gynecol Cancer*, 2012, 22, 1570–1576. [PubMed: 23051954]
9. Jensen KE, Schmiedel S, Norrild B, Frederiksen K, Iftner T and Kjaer SK, *Br J Cancer*, 2013, 108, 234–239. [PubMed: 23169283]
10. Stier EA, Engels E, Horner M-J, Robinson WT, Qiao B, Hayes J, Bayakly R, Anderson BJ, Gonsalves L, Pawlish KS, Zavala D, Monterosso A and Shiels MS, *AIDS*, 2021, 35, 1851–1856. [PubMed: 34049357]
11. Li S and Wen X, *BMC Cancer*, 2017, 17, 1–9. [PubMed: 28049525]
12. Suehiro TT, Malaguti N, Damke E, Uchimura NS, Gimenes F, Souza RP, da Silva VRS and Consolaro MEL, *Int J Gynecol Cancer*, 2019, 29, 242–249. [PubMed: 30630884]
13. Xu H-H, Yan W-H and Lin A, *Front Immunol*, 2020, 11, 1–9. [PubMed: 32038653]
14. Paaso A, Jaakola A, Syrjänen S and Louvanto K, *ACY*, 2019, 63, 148–158.
15. Tartaglia E, Falasca K, Vecchiet J, Paola Sabusco G, Picciano G, Di Marco R and Ucciferri C, *Oncol Lett*, 2017, 14, 7629–7635. [PubMed: 29344211]
16. Menon S, Rossi R, Harmon S, Mabeya H and Callens S, *Gynecologic Oncology Reports*, 2017, 22, 82–88. [PubMed: 29159260]
17. Stelzle D, Tanaka LF, Lee KK, Khalil AI, Baussano I, Shah ASV, McAllister DA, Gottlieb SL, Klug SJ, Winkler AS, Bray F, Baggaley R, Clifford GM, Broutet N and Dalal S, *The Lancet Global Health*, 2021, 9, E161–E169. [PubMed: 33212031]
18. Debeaudrap P, Sobngwi J, Tebeu P-M and Clifford GM, *Clinical Infectious Diseases*, 2019, 69, 1555–1565. [PubMed: 30602038]
19. Denslow SA, Rositch AF, Firnhaber C, Ting J and Smith JS, *Int J STD AIDS*, 2014, 25, 163–177. [PubMed: 24216030]
20. Dryden-Peterson S, Bvochora-Nsingo M, Suneja G, Efstathiou JA, Grover S, Chiyapo S, Ramogola-Masire D, Kebabonye-Pusoentsi M, Clayman R, Mapes AC, Tapela N, Asmelash A, Medhin H, Viswanathan AN, Russell AH, Lin LL, Kayembe MKA, Mmalane M, Randall TC, Chabner B and Lockman S, *J Clin Oncol*, 2016, 34, 3749–3757. [PubMed: 27573661]
21. Biggar RJ, Chaturvedi AK, Goedert JJ and Engels EA, *JNCI: Journal of the National Cancer Institute*, 2007, 99, 962–972. [PubMed: 17565153]
22. Shiels MS and Engels EA, *Curr Opin HIV AIDS*, 2017, 12, 6–11. [PubMed: 27749369]
23. Pipkin S, Scheer S, Okeigwe I, Schwarcz S, Harris DH and Hessol NA, *AIDS*, 2011, 25, 463–471. [PubMed: 21139489]
24. Castle PE, Einstein MH and Sahasrabudhe VV, *CA: A Cancer Journal for Clinicians*, 2021, 71, 505–526. [PubMed: 34499351]
25. Chambuso R, Ramesar R, Kaambo E, Denny L, Passmore J-A, Williamson A-L and Gray CM, *Journal of Cancer*, 2019, 10, 2145–2152. [PubMed: 31258717]
26. Hu JM, Sun Q, Li L, Liu CX, Chen YZ, Zou H, Pang LJ, Zhao J, Yang L, Cao YW, Cui XB, Qi Y, Liang WH, Zhang WJ and Li F, *Int J Clin Exp Pathol*, 2014, 7, 6165–6171. [PubMed: 25337265]
27. Nyagol J, Leucci E, Onnis A, De Falco G and Tigli C, *Cancer Biol Ther*, 2006, 5, 684–690. [PubMed: 16855377]
28. Barillari G, Palladino C, Bacigalupo I, Leone P, Falchi M and Ensoli B, *Oncol Lett*, 2016, 12, 2389–2394. [PubMed: 27698804]
29. Hellmuth J, Slike BM, Sacdalan C, Best J, Kroon E, Phanuphak N, Fletcher JLK, Prueksakaew P, Jagodzinski LL, Valcour V, Robb M, Ananworanich J, Allen IE, Krebs SJ and Spudich S, *J Infect Dis*, 2019, 220, 1885–1891. [PubMed: 30668739]
30. Sereti I, Krebs SJ, Phanuphak N, Fletcher JL, Slike B, Pinyakorn S, O’Connell RJ, Rupert A, Chomont N, Valcour V, Kim JH, Robb ML, Michael NL, Douek DC, Ananworanich J, Utay NS and R. 013 and S. 011 protocol teams for the RV254/SEARCH 010, *Clinical Infectious Diseases*, 2017, 64, 124–131. [PubMed: 27737952]
31. Babu H, Ambikan AT, Gabriel EE, Svensson Akusjärvi S, Palaniappan AN, Sundaraj V, Mupanni NR, Sperk M, Cheedarla N, Sridhar R, Tripathy SP, Nowak P, Hanna LE and Neogi U, *Front Immunol*, 2019, 10, 1–11. [PubMed: 30723466]

32. Micsenyi AM, Zony C, Alvarez RA, Durham ND, Chen BK and Klotman ME, *J Infect Dis*, 2013, 208, 1756–1767. [PubMed: 23908485]
33. Wang R, Simoneau CR, Kulsuptrakul J, Bouhaddou M, Travisano KA, Hayashi JM, Carlson-Stevermer J, Zengel JR, Richards CM, Fozouni P, Oki J, Rodriguez L, Joehnk B, Walcott K, Holden K, Sil A, Carette JE, Krogan NJ, Ott M and Puschnik AS, *Cell*, 2021, 184, 1–14. [PubMed: 33417857]
34. Petkov S and Chiodi F, *Genomics*, 2021, 113, 3487–3500. [PubMed: 34425224]
35. Li JZ, Arnold KB, Lo J, Dugast A-S, Plants J, Ribaudou HJ, Cesa K, Heisey A, Kuritzkes DR, Lauffenburger DA, Alter G, Landay A, Grinspoon S and Pereyra F, *Open Forum Infectious Diseases*, 2015, 2, ofu117. [PubMed: 25884005]
36. Kamat A, Misra V, Cassol E, Ancuta P, Yan Z, Li C, Morgello S and Gabuzda D, *PLOS ONE*, 2012, 7, 1–11.
37. Eckhardt M, Zhang W, Gross AM, Dollen JV, Johnson JR, Franks-Skiba KE, Swaney DL, Johnson TL, Jang GM, Shah PS, Brand TM, Archambault J, Kreisberg JF, Grandis JR, Ideker T and Krogan NJ, *Cancer Discov*, 2018, 8, 1474–1489. [PubMed: 30209081]
38. Jäger S, Cimermanic P, Gulbahce N, Johnson JR, McGovern KE, Clarke SC, Shales M, Mercenne G, Pache L, Li K, Hernandez H, Jang GM, Roth SL, Akiva E, Marlett J, Stephens M, D’Orso I, Fernandes J, Fahey M, Mahon C, O’Donoghue AJ, Todorovic A, Morris JH, Maltby DA, Alber T, Cagney G, Bushman FD, Young JA, Chanda SK, Sundquist WI, Kortemme T, Hernandez RD, Craik CS, Burlingame A, Sali A, Frankel AD and Krogan NJ, *Nature*, 2012, 481, 365–370.
39. Huang J, Qian Z, Gong Y, Wang Y, Guan Y, Han Y, Yi X, Huang W, Ji L, Xu J, Su M, Yuan Q, Cui S, Zhang J, Bao C, Liu W, Chen X, Zhang M, Gao X, Wu R, Zhang Y, Xu H, Zhu S, Zhu H, Yang L, Xu X, Zhou P and Liang Z, *J Med Genet*, 2019, 56, 186–194. [PubMed: 30567904]
40. Lou H, Villagran G, Boland JF, Im KM, Polo S, Zhou W, Odey U, Juárez-Torres E, Medina-Martínez I, Roman-Basaure E, Mitchell J, Roberson D, Sawitzke J, Garland L, Rodríguez-Herrera M, Wells D, Troyer J, Pinto FC, Bass S, Zhang X, Castillo M, Gold B, Morales H, Yeager M, Berumen J, Alvarez E, Gharzouzi E and Dean M, *Clinical Cancer Research*, 2015, 21, 5360–5370. [PubMed: 26080840]
41. Ojesina AI, Lichtenstein L, Freeman SS, Pedamallu CS, Imaz-Rosshandler I, Pugh TJ, Cherniack AD, Ambrogio L, Cibulskis K, Bertelsen B, Romero-Cordoba S, Treviño V, Vazquez-Santillan K, Guadarrama AS, Wright AA, Rosenberg MW, Duke F, Kaplan B, Wang R, Nickerson E, Walline HM, Lawrence MS, Stewart C, Carter SL, McKenna A, Rodriguez-Sanchez IP, Espinosa-Castilla M, Woie K, Bjorge L, Wik E, Halle MK, Hoivik EA, Krakstad C, Gabiño NB, Gómez-Macías GS, Valdez-Chapa LD, Garza-Rodríguez ML, Maytorena G, Vazquez J, Rodea C, Cravioto A, Cortes ML, Greulich H, Crum CP, Neuberg DS, Hidalgo-Miranda A, Escareno CR, Akslen LA, Carey TE, Vintermyr OK, Gabriel SB, Barrera-Saldaña HA, Melendez-Zajgla J, Getz G, Salvesen HB and Meyerson M, *Nature*, 2014, 506, 371–375. [PubMed: 24390348]
42. Lachkar B, Minaguchi T, Akiyama A, Liu S, Zhang S, Xu C, Shikama A, Tasaka N, Sakurai M, Nakao S, Ochi H, Yoshikawa H and Satoh T, *Medicine (Baltimore)*, 2018, 97, 1–5.
43. Gagliardi A, Porter VL, Zong Z, Bowlby R, Titmuss E, Namirembe C, Griner NB, Petrello H, Bowen J, Chan SK, Culibrk L, Darragh TM, Stoler MH, Wright TC, Gesuwan P, Dyer MA, Ma Y, Mungall KL, Jones SJM, Nakisige C, Novik K, Orem J, Origa M, Gastier-Foster JM, Yarchoan R, Casper C, Mills GB, Rader JS, Ojesina AI, Gerhard DS, Mungall AJ and Marra MA, *Nat Genet*, 2020, 52, 800–810. [PubMed: 32747824]
44. Xi R, Pan S, Chen X, Hui B, Zhang L, Fu S, Li X, Zhang X, Gong T, Guo J, Zhang X and Che S, *Oncotarget*, 2016, 7, 57050–57065. [PubMed: 27489353]
45. Chen J, *Rev Med Virol*, 2015, 25 Suppl 1, 24–53. [PubMed: 25752815]
46. Zhu J, Blenis J and Yuan J, *PNAS*, 2008, 105, 6584–6589. [PubMed: 18451027]
47. Mole S, McFarlane M, Chuen-Im T, Milligan SG, Millan D and Graham SV, *J Pathol*, 2009, 219, 383–391. [PubMed: 19718710]
48. Cerasuolo A, Buonaguro L, Buonaguro FM and Tornesello ML, *Front Cell Dev Biol*, 2020, 8, 1–24. [PubMed: 32117956]
49. Menon S, Rossi R, Zdraveska N, Kariisa M, Acharya S, Broeck D and Callens S, *BMJ Open*, 2017, 7, 1–15.

50. Kelly H, Weiss HA, Benavente Y, de Sanjose S, Mayaud P, Qiao Y, Feng R-M, DeVuyst H, Tenet V, Jaquet A, Konopnicki D, Omar T, Menezes L, Moucheraud C and Hoffman R, *The Lancet HIV*, 2018, 5, e45–e58. [PubMed: 29107561]
51. Atemnkeng N, Aji AD, de Sanjose S, Mayaud P and Kelly H, *Clin Infect Dis*, 2020, 71, e540–e548. [PubMed: 32162657]
52. Abraham AG, Strickler HD, Jing Y, Gange SJ, Sterling TR, Silverberg M, Saag M, Rourke S, Rachlis A, Napravnik S, Moore RD, Klein M, Kitahata M, Kirk G, Hogg R, Hessol NA, Goedert JJ, Gill MJ, Gebo K, Eron JJ, Engels EA, Dubrow R, Crane HM, Brooks JT, Bosch R and D'Souza G, *J Acquir Immune Defic Syndr*, 2013, 62, 405–413. [PubMed: 23254153]
53. Haga RB and Ridley AJ, *Small GTPases*, 2016, 7, 207–221. [PubMed: 27628050]
54. Zhang Y, Qian J, Gu C and Yang Y, *Sig Transduct Target Ther*, 2021, 6, 1–14.
55. Lord CJ and Ashworth A, *Nature*, 2012, 481, 287–294. [PubMed: 22258607]
56. Shi X, Wang J, Lei Y, Cong C, Tan D and Zhou X, *Molecular Medicine Reports*, 2019, 19, 4529–4535. [PubMed: 30942405]
57. Manzano RG, Catalan-Latorre A and Brugarolas A, *BMC Cancer*, 2021, 21, 1–23. [PubMed: 33397301]
58. Jiang Z, Deng T, Jones R, Li H, Herschkowitz JI, Liu JC, Weigman VJ, Tsao M-S, Lane TF, Perou CM and Zacksenhaus E, *J Clin Invest*, 2010, 120, 3296–3309. [PubMed: 20679727]
59. Williams BO, Remington L, Albert DM, Mukai S, Bronson RT and Jacks T, *Nat Genet*, 1994, 7, 480–484. [PubMed: 7951317]
60. Xu D, Zhu X, Ren J, Huang S, Xiao Z, Jiang H and Tan Y, *Journal of Proteomics*, 2022, 252, 1–8.
61. Hu Y-X, Zheng M-J, Zhang W-C, Li X, Gou R, Nie X, Liu Q, Hao Y-Y, Liu J-J and Lin B, *J Transl Med*, 2019, 17, 1–13. [PubMed: 30602370]
62. Zhao J, Guo Z, Wang Q, Si T, Pei S, Qu H, Shang L, Yang Y and Wang L, *CMAR*, 2019, 11, 7197–7210.
63. Sertznig H, Hillebrand F, Erkelenz S, Schaal H and Widera M, *Virology*, 2018, 516, 176–188. [PubMed: 29407375]
64. Pasquereau S and Herbein G, *Front Cell Infect Microbiol*, 2022, 12, 1–9.
65. Zheng Z, Cai Y, Chen H, Chen Z, Zhu D, Zhong Q and Xie W, *Front Oncol*, 2019, 8, 1–10.
66. Xiu W and Luo J, *BMC Immunol*, 2021, 22, 3. [PubMed: 33407095]
67. Huang X, Lai S, Qu F, Li Z, Fu X, Li Q, Zhong X, Wang C and Li H, *Mol Ther Oncolytics*, 2022, 25, 1–15. [PubMed: 35399607]
68. Wang J, Zhang Y, Xiao Y, Yuan X, Li P, Wang X, Duan Y, Seewaldt VL and Yu D, *Am J Cancer Res*, 2021, 11, 2005–2024. [PubMed: 34094666]
69. Hanahan D, *Cancer Discovery*, 2022, 12, 31–46. [PubMed: 35022204]
70. Carlin DE, Demchak B, Pratt D, Sage E and Ideker T, *PLoS Comput Biol*, 2017, 13, e1005598. [PubMed: 29023449]
71. Cowen L, Ideker T, Raphael BJ and Sharan R, *Nat Rev Genet*, 2017, 18, 551–562. [PubMed: 28607512]
72. Su G, Kuchinsky A, Morris JH, States DJ and Meng F, *Bioinformatics*, 2010, 26, 3135–3137. [PubMed: 21123224]
73. Csárdi G and Nepusz T, *InterJournal Complex Systems*.
74. Langfelder P, Zhang B and Horvath S, *Bioinformatics*, 2008, 24, 719–720. [PubMed: 18024473]
75. Yu G, Wang L-G, Han Y and He Q-Y, *OMICS*, 2012, 16, 284–287. [PubMed: 22455463]
76. Cerami E, Gao J, Dogrusoz U, Gross BE, Sumer SO, Aksoy BA, Jacobsen A, Byrne CJ, Heuer ML, Larsson E, Antipin Y, Reva B, Goldberg AP, Sander C and Schultz N, *Cancer Discov*, 2012, 2, 401–404. [PubMed: 22588877]
77. Gao J, Aksoy BA, Dogrusoz U, Dresdner G, Gross B, Sumer SO, Sun Y, Jacobsen A, Sinha R, Larsson E, Cerami E, Sander C and Schultz N, *Sci Signal*, 2013, 6, 1–19.
78. Gu Z, Eils R and Schlesner M, *Bioinformatics*, 2016, 32, 2847–2849. [PubMed: 27207943]
79. Auersperg N, *J Natl Cancer Inst*, 1964, 32, 135–163. [PubMed: 14114965]

80. Kim M, Park J, Bouhaddou M, Kim K, Rojc A, Modak M, Soucheray M, McGregor MJ, O'Leary P, Wolf D, Stevenson E, Foo TK, Mitchell D, Herrington KA, Muñoz DP, Tutuncuoglu B, Chen K-H, Zheng F, Kreisberg JF, Diolaiti ME, Gordan JD, Coppé J-P, Swaney DL, Xia B, van 't Veer L, Ashworth A, Ideker T and Krogan NJ, *Science*, 2021, 374, 1–18.

Author Manuscript

Author Manuscript

Author Manuscript

Author Manuscript

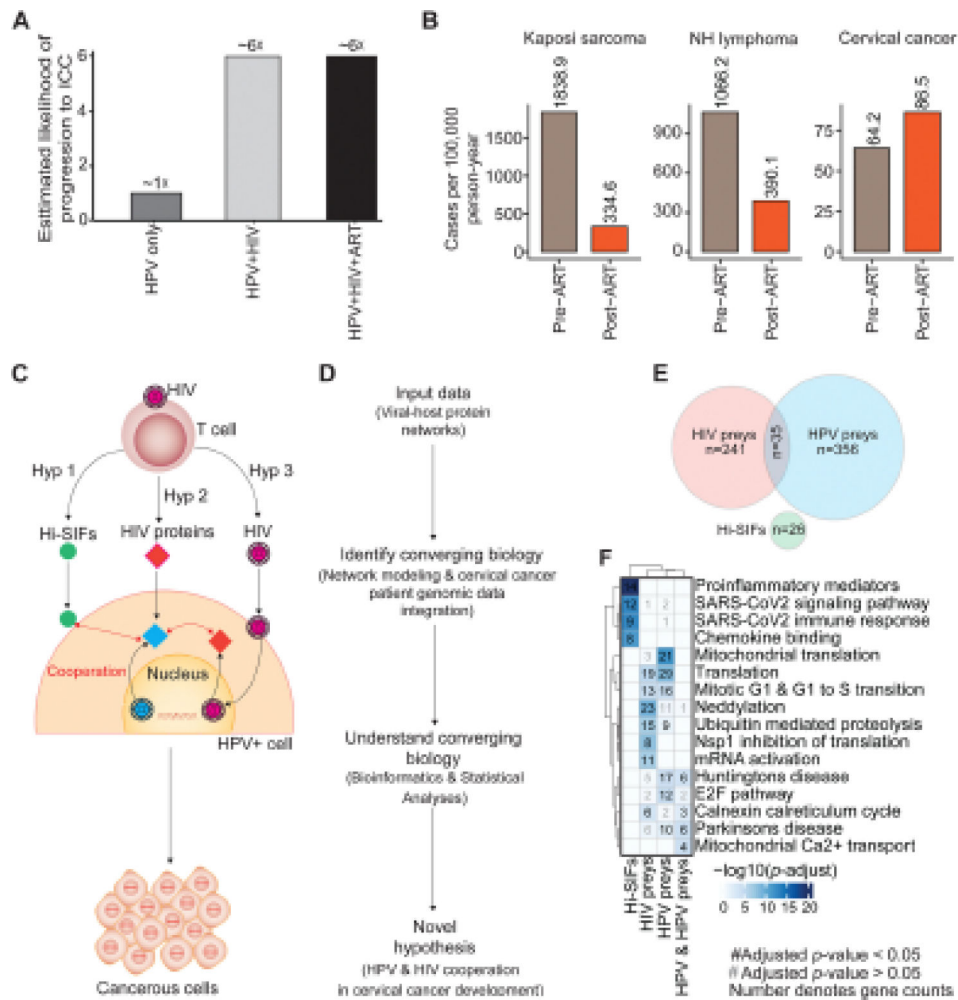


Fig. 1. Network modeling integrates molecular datasets to probe HPV/HIV cooperation in cervical cancer development.

(A) Bar plot highlighting the estimated likelihood of progression to ICC in the context of HPV, HIV/HPV coinfection and/or ART. (B) Bar plots summarizing the incidences of various HIV-associated cancers in the pre-ART (1990–1995) and post-ART (1996–2002) era. Data from Biggar et al.²¹ (C) Schematic overview of the three hypotheses that explain how HIV might be enhancing progression of HPV-associated cervical cancer. In hypothesis one, HIV infection of T cells trigger secretion of Hi-SIFs that bind to cervical cells and cooperate with HPV and its proteins. In hypothesis two, HIV-infected T cells release HIV proteins, which infiltrate cervical cells and synergize with HPV proteins. Hypothesis three involves direct infection of the cervical cells by the HIV virions from the T cells. Altogether, the cooperation between HPV/Hi-SIFs and HPV/HIV promote development of cervical cancer. (D) Schematics of the overall analysis pipeline. The analysis utilized Hi-SIFs, HPV and HIV preys as “seed nodes” which were integrated using network propagation to identify converging biology between these datasets. This was followed by bioinformatics analysis to understand converging biology and development of a novel hypothesis explaining how HPV and HIV cooperate to enhance cervical cancer development. (E) Venn diagram illustrating the overlap between and among all the Hi-SIFs, HIV, HPV preys used for analyses in this

study. Of the 33 inflammatory proteins identified from literature to be persistently expressed in HIV-infected individuals, 26 were classified as secreted proteins based on human protein atlas database (<https://www.proteinatlas.org/>) and were selected for the analyses. (F) Gene set enrichment analysis for Hi-SIFs, HIV, HPV, and HIV-HPV overlapping preys. The p -values were calculated by hypergeometric test with multiple hypothesis testing (false discovery rate; FDR). The top four pathway terms per prey category were visualized on the heatmap. A complete set of enriched biological pathways for protein categories is provided in Table S1. Hi-SIFs: HIV-induced secreted inflammatory factors; Hyp: Hypothesis

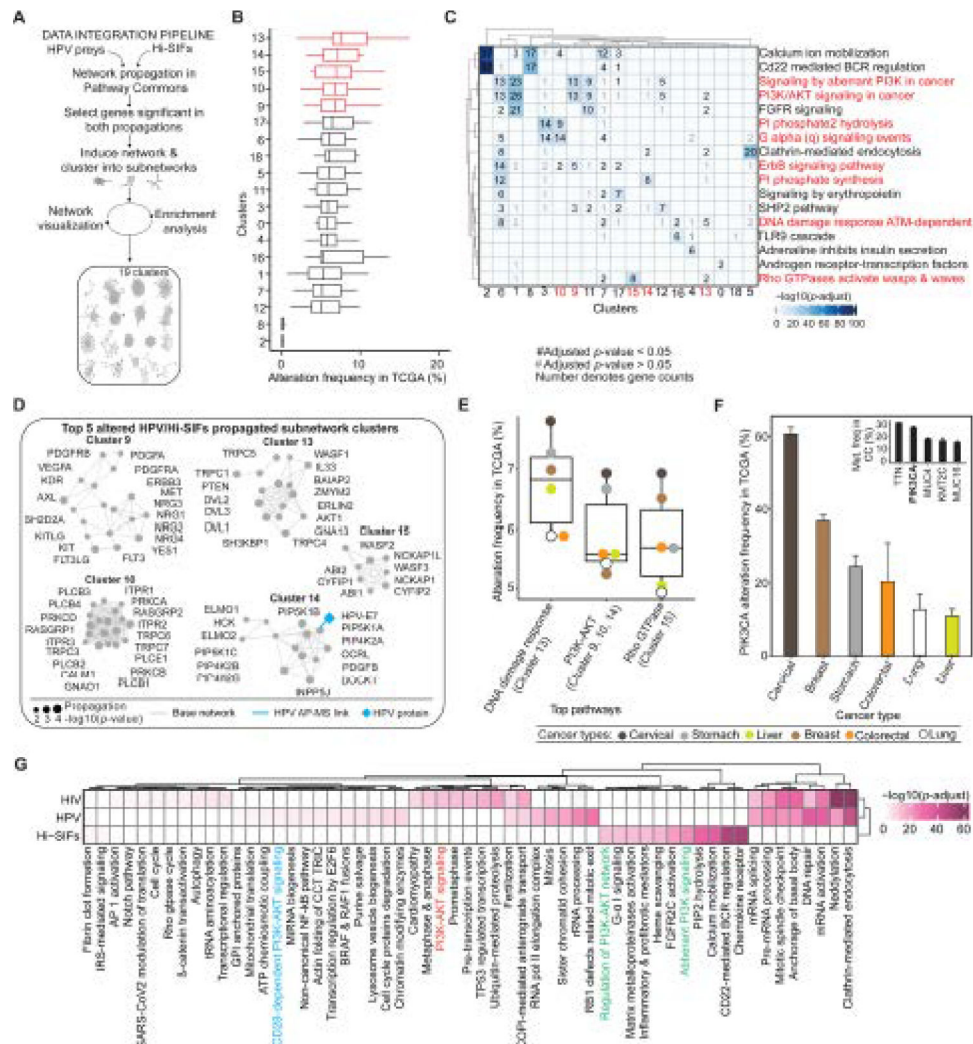


Fig. 2. Network propagation highlights host pathways co-hijacked by Hi-SIFs and HPV during cervical cancer development.

(A) Integrative network propagation pipeline for HPV preys and Hi-SIFs. Using Pathway Commons as base network, network propagation was performed independently for the Hi-SIFs or HPV preys. The propagated networks were integrated by selecting genes significant in both propagations to identify biological networks that are common between HPV and Hi-SIFs. The significant genes from the network propagation outputs were extracted, induced into subgraph, clustered into subnetwork clusters followed by gene set enrichment analysis. (B) Boxplot plot showing the alteration frequencies (including point mutations, CNA and structural variants, gene and protein expression) of genes within each subnetwork cluster in cervical cancer patients. The top five altered HPV/Hi-SIFs subnetwork clusters are highlighted in red. For each gene/node, the mean alteration frequencies for the TCGA, Pancancer Atlas and TCGA, Firehose Legacy cervical cancer studies were used. (C) A gene set enrichment analysis of the integrated Hi-SIFs/HPV propagated subnetwork clusters. The p -values were calculated by hypergeometric test with multiple hypothesis testing correction (FDR). The pathway terms associated with the top five altered clusters in cervical cancer patients identified in (B) are highlighted in red. A complete set of enriched biological

pathways is provided in Table S2. **(D)** The networks of the top five altered subnetwork clusters identified in (B and C). All the 19 subnetwork clusters are shown in Fig. S1. **(E)** Comparison of the alteration frequencies (including point mutations, CNA and structural variants, gene and protein expression) of nodes of the top five altered clusters grouped based on the pathways they are implicated in across common cancers among women. Each dot represent the mean alteration frequencies from the TCGA, Pancancer Atlas and TCGA, Firehose Legacy studies for the respective cancer types. **(F)** Alteration frequencies (including point mutations, CNA and structural variants, gene and protein expression) of PIK3CA, a key node in the PI3K pathway across common cancers among women. Bars represent the mean alteration frequencies for the TCGA, Pancancer Atlas and TCGA, Firehose Legacy studies for the respective cancer types. The inset depicts the top five mutated genes in cervical cancer patients. Data shown are the mean mutation frequencies from the two cervical cancer studies (TCGA, Pancancer Atlas and TCGA, Firehose Legacy) curated in cBioPortal. Error bars represent the standard error of the mean. **(G)** A heatmap showing the top term per subnetwork cluster generated from HPV preys, Hi-SIFs and HIV preys propagation outputs. The top 500 genes from the individual propagations per dataset (HPV only, Hi-SIFs, HPV only) were extracted and induced into a network, clustered into subnetwork clusters followed by gene set enrichment analysis. The p -values were calculated by hypergeometric test with multiple hypothesis testing correction (FDR). Complete enrichment tables used to generate the heatmap are provided in Table S3–S5. CC: Cervical cancer, Mut: Mutation; TCGA: The Cancer Genome Atlas

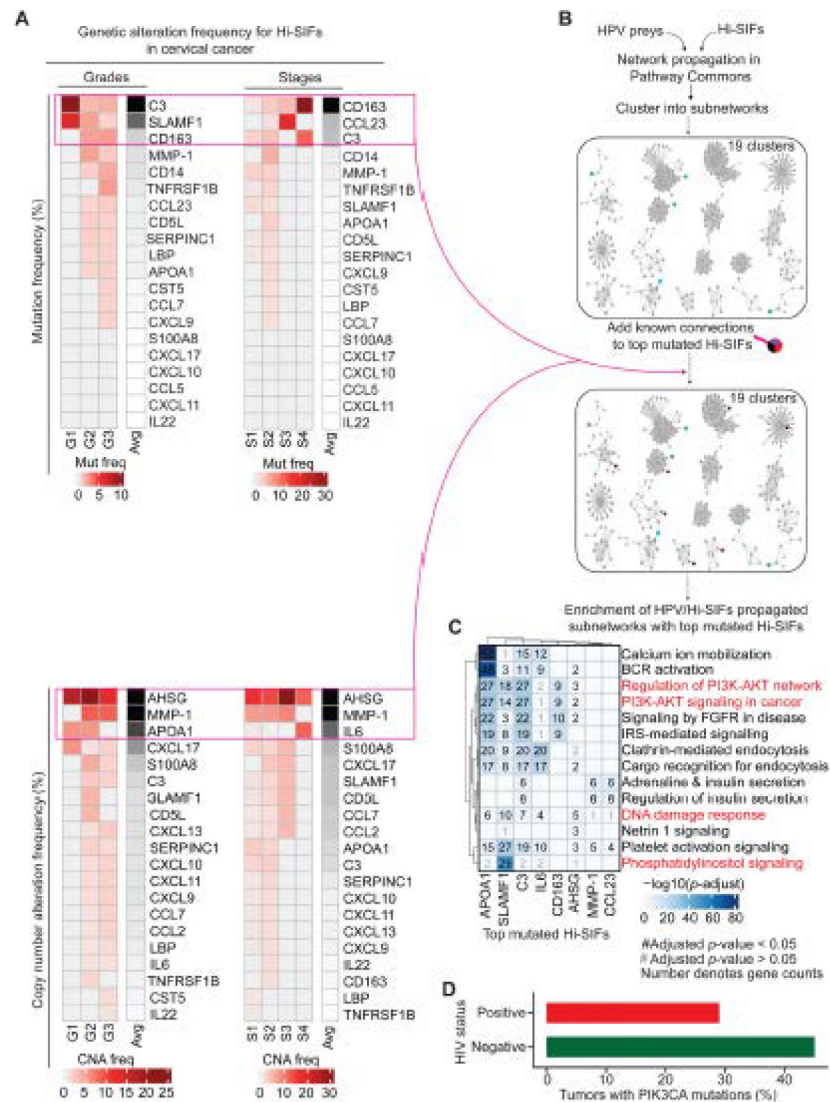


Fig. 3. Cervical cancer genomics reveal Hi-SIFs converge on PI3K-AKT signaling pathway, representing HIV-mediated phenocopy of PI3K-AKT pathway mutations. (A) Ranked mutation and copy number alteration (CNA) frequencies of Hi-SIFs across different cervical cancer grades and stages from the cBioPortal and the top three mutated Hi-SIFs that were selected for integration into the HPV/Hi-SIFs propagated network. For each Hi-SIF, the mean mutation or CNA frequency from the TCGA, Pancancer Atlas and TCGA, Firehose Legacy cervical cancer studies were used. (B) Integration of the top mutated Hi-SIFs into the HPV/Hi-SIFs propagated subnetwork clusters. The top mutated Hi-SIFs were overlaid onto the HPV/Hi-SIFs propagated network by establishing known connections between each of them and the genes within the subnetwork clusters using Pathway Commons networks. (C) Gene set enrichment analysis for propagated Hi-SIFs/HPV subnetwork clusters with connections to the top mutated Hi-SIFs. The pathways that are in line with the top five mutated clusters from Fig. 2C are highlighted in red. A complete set of enriched biological pathways for the Hi-SIFs/HPV subnetwork clusters connected to the top mutated Hi-SIFs are listed in Table S7. (D) Bars showing

the percentage of HIV-positive and HIV-negative tumors with PIK3CA mutations from a Ugandan cohort of cervical cancer patients. Data from Gagliardi et al.⁴³

Author Manuscript

Author Manuscript

Author Manuscript

Author Manuscript

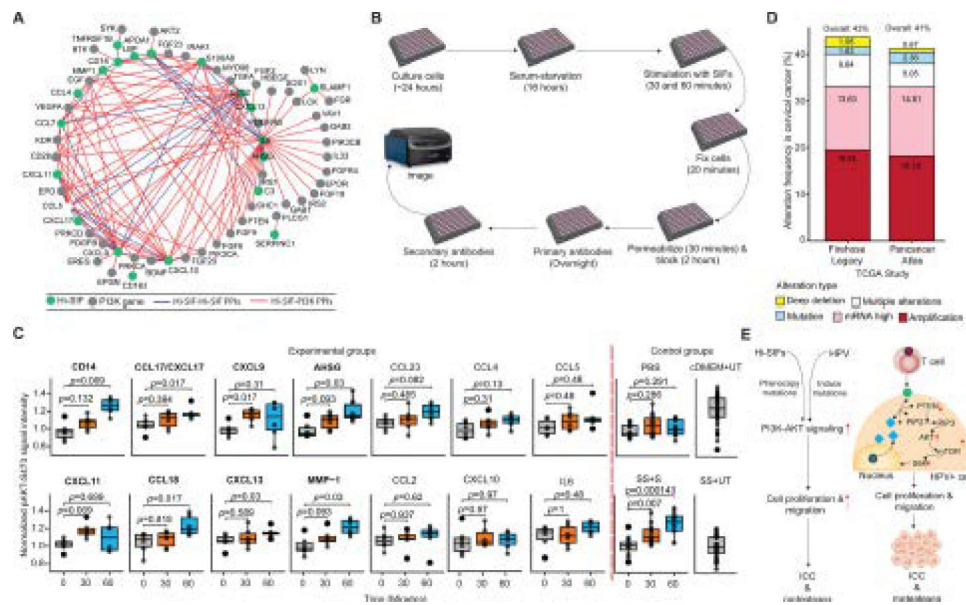


Fig. 4. Mechanistic model explaining HIV and HPV cooperation in cervical cancer development. (A) Network showing how the Hi-SIFs and the top 100 significant PI3K pathway genes from Hi-SIFs/HPV network propagation interact with each other, annotated from Pathway Commons network and visualized in Cytoscape. (B) Workflow showing the in-cell western blot assay procedure that was used to quantify the levels of pAkt-S473 as proxy for PI3K pathway activation upon stimulation of C33A cell line with different Hi-SIFs for 30 or 60 minutes. The cells were grown confluence, serum-starved and stimulated for 30 or 60 minutes. Cells were then fixed and stained with primary and secondary antibodies before imaging. (C) Levels of pAkt-S473 as measured by in-cell western blot assay upon stimulation of C33A cells with Hi-SIFs. Box plots depict the median intensity of pAKT normalized to levels of pAKT of serum-starved cells per plate and upper and lower quartiles of the distribution whereas the whiskers represent 1.5 times the interquartile range. Statistical comparisons between time 0 versus 30 or 60 minutes were performed using Wilcoxon test. Dots (n=6) in each box plot represent technical duplicate wells per plate for three independent plates. The p-adjust are displayed. Hi-SIFs with at least one significant ($p < 0.05$) comparison are highlighted in boldface. (D) Bar plot showing the percentage alteration frequencies (including point mutations, CNA and structural variants, gene and protein expression) of the 8 Hi-SIFs significantly elevating pAKT in (C) among cervical cancer patients listed in cBioPortal. The overall alteration frequencies associated with these Hi-SIFs for TCGA, Firehose Legacy and TCGA, Pancancer Atlas cervical cancer studies are displayed on top of the bars. Data from cBioPortal. (E) Model showing how HIV and HPV infections alter PI3K-AKT signaling. In the context of coinfection, both HPV proteins and HIV-induced SIFs activate PI3K signaling pathway leading to aberrant cell proliferation and migration thereby enhancing progression to ICC and metastasis.